

ASSESSMENT OF SHEAR STRENGTH PARAMETERS OF SEDIMENTARY INTACT ROCK SPECIMENS AS A FUNCTION OF DEGREE OF SATURATION

Amjad Ibrahim Fadhil¹, Ahmed Ibrahim Fadhil Al-Adly², *Ahmed S.A. Al-Gharbawi³, Mohammed Y. Fattah⁴

¹Department /or Faculty, University, Country Department of Production Engineering and Metallurgy, University of Technology-Iraq, Baghdad, Iraq; ²Department of Civil Engineering, Al-Rafidain University College, Baghdad, Iraq; ^{3,4} Civil Engineering Department, University of Technology-Iraq, Baghdad, Iraq.

*Corresponding Author, Received: 21 Nov. 2022, Revised: 12 Dec. 2022, Accepted: 02 April 2023

ABSTRACT: Rock cracks are the end consequence of a masses of the rock failing in tension, shear, or a amalgamation of the two. Depending on how the machinery works that created the fissures and some of the rock, two forms of fissure morphology—dry or saturated fissures—may be visible (water-filled fissures). The goal of the current work is to develop a connection between the strength characteristics of intact rock specimens and the variation in water content. A new mathematical method was developed to find the relationship between cohesion (c), angle of internal friction (ϕ), uniaxial compressive strength (UCS), and the degree of saturation variation. A series of experimental tests were carried out on (100) intact rock specimens collected from the Ayoun al-Shajij region which is located West of Najaf province central of Iraq. According to the Mohr-Coloumb failure criterion, a new expression was developed to find the relationship between the shear strength parameters and water content of rock samples. According to the results, there is a linear and exponential relationship between increasing rock saturation and a reduction in the parameters of the shear strength (c and ϕ). In order to link the cohesiveness and angle of friction to the rock's saturation level, new expressions have been found to be useful. While the angle of internal friction demonstrated a negative linear association with the degree of saturation, the cohesion demonstrated a negative important relation with the increase in saturation point.

Keywords: Shear strength, Rock, Saturation, Uniaxial strength.

1. INTRODUCTION

When designing a structure on top of or inside of the rock, the strength and deformability properties of the intact rock play a critical role in the classification of the rock type. In many cases, the engineering performance of a rock mass under external loadings is dictated by the strength and direction of the discontinuities rather than the characteristics of the whole rock. Other factors that influence rock behavior are the presence of water and the initial stresses within the rock mass which can decrease the parameters of the shear strength.

The relationship between the existence of water content and some mechanical and physical characteristics of rock has been the subject of several recent investigations. The strength and deformability of rocks are significantly influenced by water, as is widely known. A slight increase in the amount of water may result in a significant loss of strength [1 - 5].

Hawkins and McConnell [1] examined the amount of water that was present in 35 different varieties of British sandstone that were collected from 21 different locations and dated from the Pre-Cambrian to the Cretaceous. They provided information on the measured uniaxial compressive

strength as well as the tangent and secant deformation moduli under both saturated and dry conditions.

The conditions of the rock are affected by excavation as well as the direct mechanical effects (qualities that are mechanical, hydraulic, and chemical). The internal fluids, and especially the amount of water present in the rock, could be considerably changed in connection to hydration and desiccation. Valès et al. [6] studied the effect of the saturation point and the mechanical and physical features of Tournemire shale rock relate to one another. Regulated suctions are used to impose different amounts of soaking while continuously measuring physical traits like weight and deformations. The opening or closing of the interlayer space would be the primary cause of the volume changes (swelling or shrinking behavior). The association between a number of mechanical parameters (elasticity and fracture data) and sample saturation was established through the use of uniaxial and triaxial compressive testing. The stratification, as well as how it is oriented in relation to the mechanical stress, has a big impact on the mechanical behavior, which is dependent on the shale's saturation point.

Both the dried and fully saturated uniaxial

compressive strengths are correlated with one another, c_0 and c_{sat} , according to Vasarhelyi [2], who conducted an analysis of the data that had already been reported. Vasarhelyi and Van [3] examined the relationship between the variation in compressive or tensile structural strength and water content and found that it exhibits a sharp fall for low water content and maintains a practically constant rate for higher moisture content. Up to 70%, less can be found in the saturated ultimate strengths than in the dry one. Igneous and metamorphic rocks are less resistant to water than sedimentary rocks, according to Wong et al. [7].

In the study by Yao et al. [8] on the influence of water content on the mechanical characteristics of coal and fine-grained sandstone, respectively, it was discovered that the elastic modulus had an inverse exponential relationship with moisture content. When the water content grew, the post-peak modulus and strain softening parameter decreased. Although the post-peak modulus and the strain relaxation parameter exceeded the elastic modulus by two orders of magnitude, the resistance to deformation during the post-peak period was lower than that experienced during elastic deformation.

In their study, Khosravi et al. [9] developed a novel testing approach that was created to assess the hydro mechanical performance of the filled rock fissures during mechanical hysteresis. The experimental strategy included the following three steps: (1) using the axis interpretation technique to modify a triaxial test instrument for suction control; (2) using a discharge piston to precisely measure the infill degree of saturation, S_r ; and (3) that use a method for analyzing digital images to determine the filler materials' volume changes and the fracture dilatancy under shear. A suction-feedback control loop with a pressure transducer was employed during the test to regulate the flow of water toward or away from the specimen in order to create suction equilibrium conditions.

The experimental data were presented and addressed on a variety of topics crucial to the evaluation and interpretation of their in-situ reaction, according to Ventini et al. [10]. In the experiment, samples of two different types of gravel with the same grade were reconstituted at the same starting relative density and put through three series of oedometer testing. Focusing on the significance of saturation level (S_r) through evaluation of the "driest," "totally saturated," and transitional conditions, this presentation, and discussion of experimental findings on the compressibility of rockfills emphasize this. Tests on soil particles that have been both dry and soaked with water are also included for grain crushing. The findings demonstrated that, particularly in rockfill/stress settings that are prone to crushing, it is hard to overlook the effect of S_r when evaluating the

material's mechanical properties.

In relation to the level of saturation (S_r) and water distribution within the pore network, Rabat et al. [11] investigated the mechanical characteristics of three different types of calcarenite, including the Uniaxial Compressive Strength, Young's modulus, Brazilian Tensile Strength, and Point Load Strength Index. In order to achieve this, specimens made using two distinct wetting procedures and various S_r values were put through the associated mechanical testing and magnetic resonance imaging methodology over a period of time. The findings indicated that specimens moistened through the drying process exhibit larger losses in mechanical properties than specimens soaked during the immersion method for low S_r levels (50%), but the declines are about equivalent for both wetting techniques for higher S_r values (> 50%). Furthermore established, albeit with some modest variations, were correlation matrices that compared the mechanical characteristics of specimens soaked using each of the wetting techniques.

By using models tested numerically that can precisely represent the variable elastic and plastic anisotropy with DOS, it is required to predict the structural properties of kaolin rocks in partially soaked environments. In unsaturated elastoplastic media, a coupled solid deformation-fluid flow anisotropic framework was presented by Sabrina and Borja [12]. An anisotropic modified Cam-Clay (MCC) model was used to take into account the increasing strength anisotropy as well as the asymmetry of the elastic and plastic reactions. To show that the model can accurately explain strength anisotropy at various saturation points, using experimental information from triaxial testing, it was calibrated. It was shown through numerical simulations how the mechanical properties behavior of kaolin rocks changed when the strength and stiffness anisotropy increased. Triaxial compression tests were also carried out under models of plane strain to show how material anisotropy and DOS affect the mechanical and fluid flow responses.

2. RESEARCH SIGNIFICANCE

Saturation-dependent physical anisotropy must be taken into account in the method to calculate of rock behavior for applications that involve wetting and/or drying processes, which including tunnel building or underground nuclear waste storage. For the current experiment, a novel method based on the Mohr-Coulomb failure criterion was developed in effort of establishing a connection between the degree of saturation of rock layers and the shear strength indices (c and ϕ). To explain the strength of a rock sample, it will be necessary to determine its water content or level of saturation.

3. EXPERIMENTAL WORK

This section covers the location, geology, and number of rock specimens obtained from the study region, as well as how those specimens were prepared. In addition, a summary of the tests conducted is provided, together with information on the physical, destructive, and non-destructive tests.

3.1 Geology of the Study Area

The samples of the rock are collected from the study area of Ayoun al-Shajij which is located to the west of Al-Najaf province central of Iraq within the formation of the Limestone Euphrates. It is located 26 km from the center of the province, and an area estimated (at 16) km² is located within the coordinates (E 42 72 22.7), (N 32 25 18.1) / (E 42 64 05.1), (N 32 21 44.4). The locations from which rock samples were collected are shown in Fig. 1 together with the geology map of the study region.

3.2 Sample Preparation

As shown in Fig. 2, the block rock samples were drilled and cut into cylinder and disc samples with various height-to-diameter ratios in accordance with the test type. The unconfined compressive strength (UCS) test samples are cylinder specimens which is standard dimensions

that were prepared according to (ASTM D4543) [15], Fig. 3. Brazilian test (BT) samples are disc samples which were prepared according to (ASTM D3967-95a) [16], Fig. 4. Table 1 shows the details of rock samples used in the experiments. The rock samples are dried by using an oven in soil mechanics laboratory at (1105°C) for 24 hours in accordance with (ASTM D2216-98) [17] in this investigation. Whole dry samples were employed in the study before testing.

Table 1 Dimensions of specimens of rock.

Average diameter (mm)		Average t, L (mm)	
B.T	UCS	B.T	UCS
54	54	24	110

3.3 Physical Tests

The laboratory physical tests were conducted on rock samples. The physical properties are important in the assessment of rocks, including total density, virtual qualitative weight, absorption ratio, and appearance-specific gravity. The tests were carried out according to the American specification, ASTM C568-03 [18]. The results of the physical laboratory tests are summarized in Table 2.

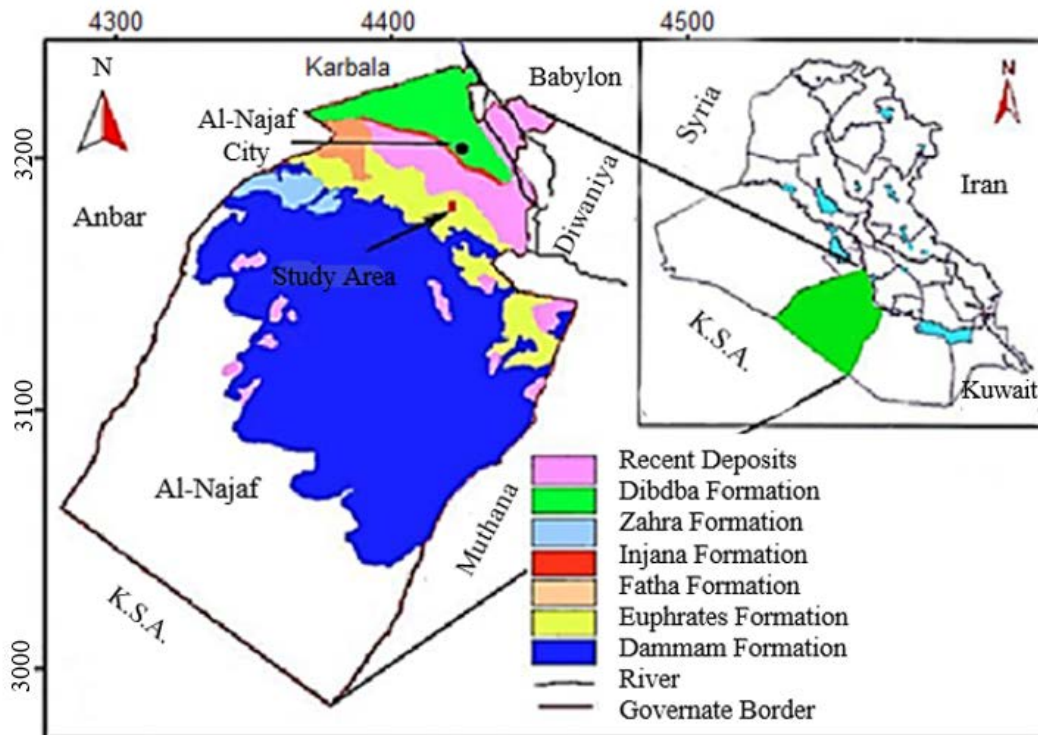


Fig. 1 Placement and a geographical map of the research area [13, 14].



Fig. 2 Block samples cored.

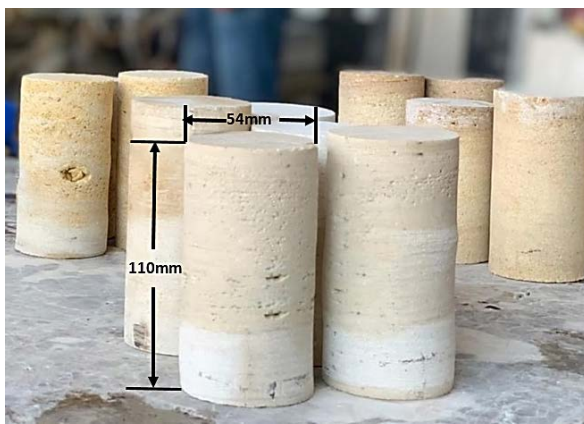


Fig. 3 Unconfined compression test specimens.



Fig. 4 Brazilian test specimens.

Table 2 Summary of physical tests.

Test	Average value	ASTM
Bulk Density (g/cm ³)	2.34	
Porosity (%)	6.89	ASTM C
Void ratio (%)	7.39	97-02,
Apparent Specific Gravity	2.59	2003 [19]
Water Absorption (%)	3.07	

3.3.1 Saturation of specimens

The specimens were weighed, dried for 24 hours at 106 °C, then re-weighed to set the fully dry

weight in order to ascertain the impact of water saturation on the mechanical properties of rocks. A dry sample was submerged in a tank of purified water for varying lengths of time as part of the saturation procedure, and it was then removed and weighed. Every day until the specimen's weight remained constant, the procedure was repeated. The specimen had reached its saturation point at this point. The moisture content of the sample was assessed at various stages using the weight increase. After 406 hours of immersion, the change in the weights of the samples came to a standstill. The water content was obtained based on ASTM D2216 [17], the Eq. (1) and Eq. (2) were used to find the percentage of water content as follows. Fig. 5 shows the relationship between water content and time of immersion.

$$w_c = \frac{m_w - m_d}{m_d} * 100 \quad (1)$$

$$s_r * e = G_s w_c \quad (2)$$

where w_c (%) is the moisture content of the sample, m_w (g) and m_d (g) are the moist mass and dry mass of the sample, respectively, S_r (%) is the degree of saturation, e void ratio, and G_s specific gravity of rock specimen.

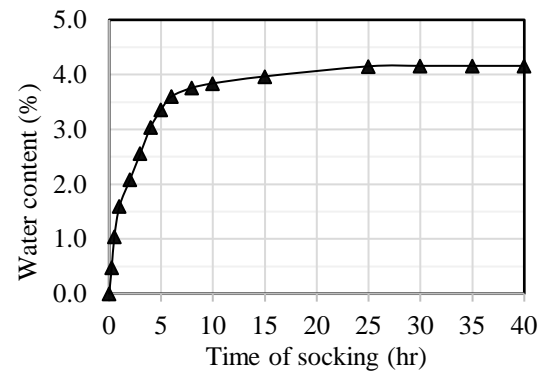


Fig. 5 Variation of water content with the time of soaking.

3.3.2 Unconfined Compression Test

On samples that were prepared at various levels of saturation, 25 (UCS) tests were run (0, 25, 50, 75, and 100%). The tests were conducted using the WDW-200E electronic universal testing machine shown in Fig. 6. The specimen can be subjected to a compression vertical load with a rate of strain remains constant to the machine's maximum capacity of 3000 kN. The test was conducted following the applicable ASTM standard practice (ASTM D 7012-e1) and the specimens were prepared [20]. The length-to-diameter (L/D) ratio of each specimen is 2.0, and they were all gradually loaded till reach the failure at a steady rate of (0.5

MPa/sec). The applied force is regarded as the failure load when a substantial displacement is seen as a result of a minor increase of the applied load (pf). The correlation between uniaxial compressive strength and saturation level is depicted in Fig. 7. The unconfined compressive strength decreases as the saturation level rises, as can be shown. The UCS decreases by about 44% when the sample is changed from dry to fully saturated. The following Eq. (3) expressions could be obtained with a coefficient of correlation $R^2 = 0.9377$:

$$UCS = 50.4 - 0.148 S \quad (3)$$

3.3.3 Brazilian Test

A total of fifty tests were conducted for various levels of saturation (0, 25, 50, 75, and 100%). The preparation of the sample and the testing technique adhere to the relevant ASTM standard practice (ASTM D 3967 - 95a) [16]. The t/D ratio of all specimens was 0.5. The test was conducted utilizing a Brazilian test device. According to the procedures depicted in Figs. 8 and 9, The samples were loaded till failure while being supported by two steel jaws. For these two flanges to cause tensile fracture along the specimen's vertical breadth diameter, the load must operate tangentially to the disc-shaped specimen. So that the load indicator displays the maximum value of the load digitally. In Fig. 10, it is depicted that the BTS tensile strength test and the saturation level have a link. The BTS tensile strength decreases as the saturation level rises, as can be shown. The tensile strength decreases by about 230% when the sample is changed from dry to fully saturated. Between 0 and 25% saturation, the majority of the strength was either lost or the linear strength loss with increasing saturation. The value of Brazilian tensile strength (BTS) was obtained using Eq. 4 [21]. And Eq. 5 showed relation could be obtained with a coefficient of correlation $R^2=0.9858$.

$$BTS=2F/\pi Dt \quad (4)$$

$$BTS= 3.7791 * e^{-0.013 S} \quad (5)$$

where:

BTS= Brazilian tensile strength (MPa), F =Failure load (N), D= specimen diameter (mm), and t= specimen thickness (mm).

4. METHODOLOGY OF THE PROPOSED PROCEDURE

According to experimental results and the Mohr-Coulomb failure criterion for the uniaxial compressive strength test shown in Fig. 11, the value of (σ_c) can be determined as shown in Eq. 6.

$$\sigma_c = \frac{2C\cos\phi}{1-\sin\phi} \quad (6)$$



Fig. 6 WDW-200E electronic universal testing machine.

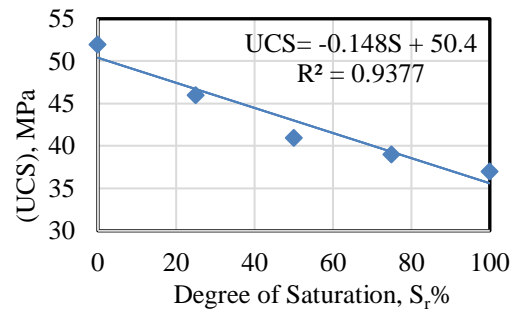


Fig. 7 Relationship between degree of saturation and uniaxial compressive strength of rock samples.



Fig. 8 Brazilian test jaws



Fig. 9 Brazilian test apparatus.

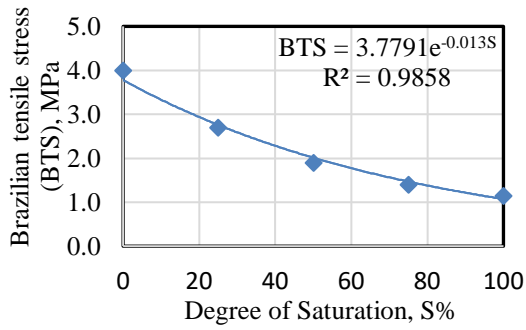


Fig. 10 Relationship between degree of saturation and uniaxial compressive strength of rock samples.

Referring to the value of indirect tensile strength (σ_t) obtained from the Mohr-Coulomb failure criterion as shown in Fig. 12 and Eq. 7.

$$\sigma_t = \frac{c \cos \phi}{2 - \sin \phi} \quad (7)$$

By divided Eq. 6 on Eq. 7:

$$\frac{\sigma_{c-uns.}}{\sigma_{t-dry}} = \frac{2(2 - \sin \phi)}{1 - \sin \phi} \quad (8)$$

Assume $\frac{\sigma_{c-uns.}}{\sigma_{t-dry}} = \Psi$, where Ψ is a new factor and can be determined for all degrees of saturation as shown in Eqs. 9 - 12.

$$\Psi = \frac{2(2 - \sin \phi)}{1 - \sin \phi} \quad (9)$$

$$\Psi - \Psi \sin \phi = 4 - 2 \sin \phi \quad (10)$$

$$(\Psi - 2) \sin \phi = \Psi - 4 \quad (11)$$

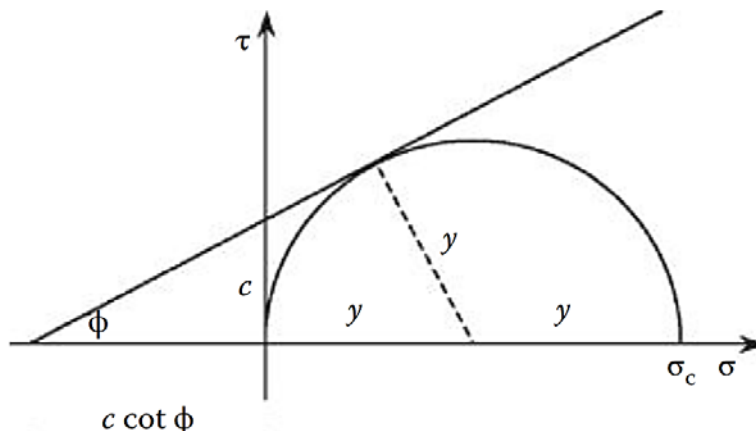


Fig. 11 Mohr circle at failure at uniaxial compressive strength test.

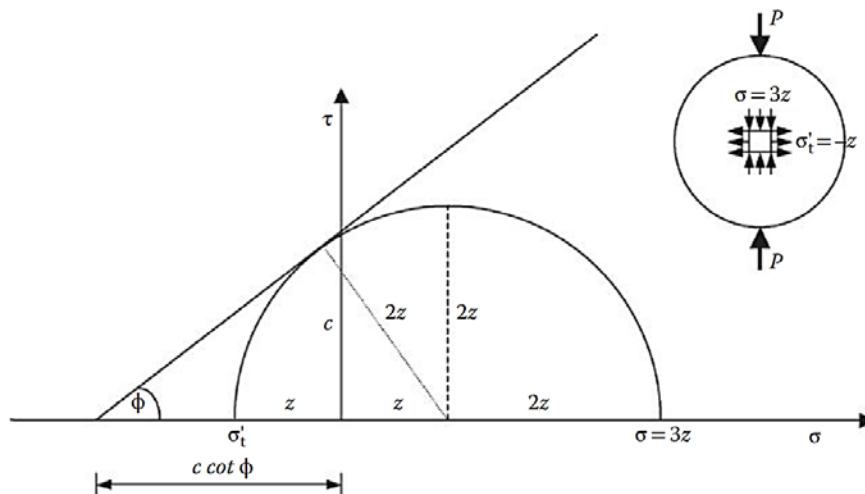


Fig. 12 Mohr circles for the element at the center of the specimen during failure in a Brazilian indirect tensile strength test.

$$\sin\phi = (\Psi-4)/(\Psi-2) \quad (12)$$

Then eqs. above are used to find the value of cohesion, *c*. Figs. 13 and 14, show the relationships between the shear strength parameters, (*c* and ϕ) and the degree of saturation based on the above equations. The results show exponentially the decrease in cohesion value with a degree of saturation. The results also show a linear decrease in the value of the angle of internal friction when the degree of saturation increases. The variation of cohesion and angle of internal friction with the degree of saturation can be expressed in the eqs. 13 and 14 relations with $R^2 = 0.908$ and 0.9441 , respectively.

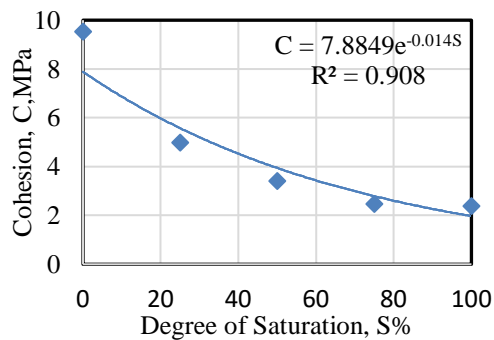


Fig. 13 Relationship between cohesion and degree of saturation.

$$c = 7.8849 * e^{-0.014 S_r} \quad (13)$$

$$\phi = 48.332 - 0.0917 S_r \quad (14)$$

The findings show a clear relationship between strength decreases between the dry and saturated states as well as substantial trends in the decline of unconfined compressive strength with increasing saturation levels. Compared to sandstones of medium to low strength, which has less consistent behavior, Abdul Shaoor and Barefield [22] found that the same tendencies are more constant for high-strength sandstones.

The limitations of performing in-situ testing protocols on rock masses make them unsuitable for site studies for hydropower projects in open terrains very frequently [23]. It is important to obtain sufficient upward reaction for the projected structural loads, which are typically of higher magnitude, in order for these tests to be carried out and for better engineering decisions to be made. In order to be on the safe side, these loads must be multiplied by at minimum 1.5 to 2 times the

expected design loads. The crown reaction from the cover is enough to satisfy this criterion, especially in drift zones (small audits). The current manuscript deals with situations that arose when conducting necessary testing in tough open terrains, and it makes site-specific recommendations for how to resolve them using the tools at hand.

Between the dry and saturated stages, the sandstones' unconfined compressive strength significantly decreased (by up to 71.6%), according to Barefield and Abdul Shaoor's findings [24]. Sandstones with higher compressive strength and lower absorption show a linear, consistent decline in unconfined strength as saturation levels rise. For weak sandstones, the preponderance of unconfined compressive strength is reduced between 0% and 20% saturation, while there are only slight or irregular strength losses at higher saturation levels.

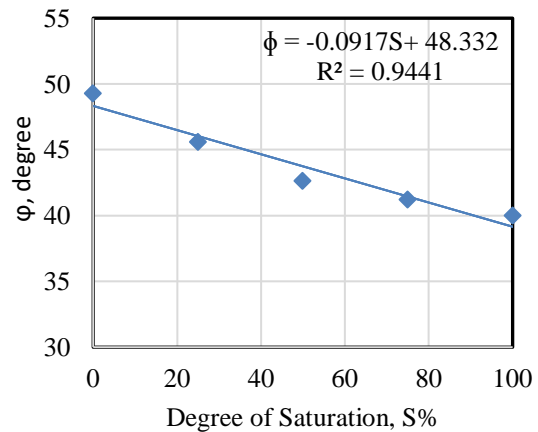


Fig. 14 Relationship between angle of internal friction and degree of saturation.

5. LIMITATIONS

The current effort is not an exhaustive investigation. It is constrained to the set of factors specifically examined to calculate the shear strength of rock specimens. The study that has been done so far has not taken into account additional factors that affect how rocks behave.

6. CONCLUSIONS

The current effort is not an exhaustive investigation. It is constrained to the set of factors specifically examined to calculate the shear strength of rock specimens. The study that has been done so far has not taken into account additional factors that affect how rocks behave.

7. REFERENCES

- [1] Hawkins A.B., McConnell B.J., Sensitivity of sandstone strength and deformability to changes in moisture content. *Q. Eng. Geol.*, Vol. 25, 1992, pp. 115–130.
- [2] Vasarhelyi B., Statistical analysis of the influence of water content on the strength of the Miocene limestone. *Rock Mech. Rock Engng.*, Vol. 38, No. 1, 2005, pp. 69-76.
- [3] Vasarhelyi B. and Van P., Influence of water content on the strength of rock. *Engineering Geology*, Vol. 84, No. 1-2, 2006, pp. 70- 74.
- [4] Torok A. and Vasarhelyi B., The influence of fabric and water content on selected rock mechanical parameters of travertine, examples from Hungary. *Engineering Geology*, Vol. 115, No. 3-4, 2010, pp. 237-245.
- [5] Yilmaz I., Influence of water content on the strength and deformability of gypsum. *International Journal of Rock Mechanics & Mining Sciences*, Vol. 47, No. 2, 2010, pp. 342-347.
- [6] Valès F., Minh D. M., Gharbi A., Rejeb A., Experimental study of the influence of the degree of saturation on physical and mechanical properties in Tournemire shale (France)", *Applied Clay Science*, Vol. 26, Issues 1–4, 2004, pp. 197-207. <https://doi.org/10.1016/j.clay.2003.12.032>.
- [7] Wong L.N.Y.; Maruvanchery V., Liu G., Water effects on rock strength and stiffness degradation. *Acta Geotech.* Vol. 11, 2016, pp. 713–737.
- [8] Yao W.Y., Shi M. L., Wu Z. R., Wang L. J., Yang C.Q., Management technology and demonstration effect on the two-dimensional configuration in Pisha Sandstone area Yellow River, Vol. 38, No. 6, 2016, pp. 1-7 (in Chinese).
- [9] Khosravi A., Serej A. D., Mousavi S. M., Haeri S. M., Effect of hydraulic hysteresis and degree of saturation of infill materials on the behavior of an infilled rock fracture, *International Journal of Rock Mechanics and Mining Sciences*, Vol. 88, 2016, pp. 105-114. <https://doi.org/10.1016/j.ijrmms.2016.07.001>.
- [10] Ventini R., Flora A., Lirer S., Mancuso C. and Cammarota A., An experimental study of the behaviour of two rockfills accounting for the effects of degree of saturation, 4th European Conference on Unsaturated Soils (E-UNSAT 2020), E3S Web of Conferences, Vol. 195, 2020. <https://doi.org/10.1051/e3sconf/202019503033>.
- [11] Rabat A., saturation and water distribution in mechanical behaviour of calcarenites using magnetic resonance imaging technique, *Construction and Building Materials*, Vol. 303, 2021. <https://doi.org/10.1016/j.conbuildmat.2021.124420>.
- [12] Sabrina C.Y., Borja R.I., Evolution of anisotropy with saturation and its implications for the elastoplastic responses of clay rocks, *Numerical and Analytical Methods in Geomechanics*, Vol. 46, No. 1, 2022. <https://doi.org/10.1002/nag.3289>.
- [13] Al-Auweidy M.R.A., Qualitative, Quantitative and Radiological Assessment of Marl Layer in the Euphrates Formation for Portland Cement Industry in Kufa Cement, Quarry at Al-Najaf Governorate", M.Sc. Thesis, University of Baghdad- College of Science, 2013.
- [14] Sissakian V.K., *Geological Map of Iraq*", 3rd edition, scale 1: 1 000 000, Geosurve, Baghdad, Iraq, 2000.
- [15] ASTM D4543, Standard Test Method for Preparing Rock Core as Cylindrical Test Specimens and Verifying Conformance to Dimensional and Shape Tolerances, 2003.
- [16] ASTM D3967 – 95a, Standard Test Method for Splitting Tensile Strength of Intact Rock Core Specimens, 2001.
- [17] ASTM D2216 – 10, "Standard test methods for laboratory determination of water (moisture) content of soil and rock by mass", American Society for Testing and Materials, 2005.
- [18] ASTM C568-03 Standard Specification for Limestone Dimension Stone, American Society for Testing and Materials, 2003.
- [19] ASTM C 97-02, 2003, Standard test methods for absorption and bulk specific gravity of dimension stone. *Annual Book of ASTM Standard American Society for Testing and Materials*. Vol.04.07, 2007.
- [20] ASTM D7012-07e, Standard test method for compressive strength and elastic moduli of intact rock core specimens under varying states of stress and temperatures, 2007.
- [21] Gokhale K., *Experiments in Engineering Geology*". Tata McGraw-Hill, New Delhi, 1960, pp. 23–32 and pp. 47–49.
- [22] Abdul Shaoor and Barefield E.H., Relationship between Unconfined Compressive Strength and Degree of Saturation for Selected Sandstones, *Environmental & Engineering Geoscience*, Vol. 15, No. 1, 2009, pp. 29–40. <https://doi.org/10.2113/gseegeosci.15.1.29>.
- [23] Ramana G.V., Mogha A.A.B., Pathak S., Reappraisal on the Field Tests for Determination of Rock Mass Characteristics for Open Terrain (s), *Proceedings of the Indian Geotechnical Conference, Lecture Notes in Civil Engineering*, Vol. 137, 2019, pp. 711-721. https://doi.org/10.1007/978-981-33-6466-0_66.

- [24] Barefield E. H., The effect of degree of saturation on the unconfined compressive strength of selected sandstones, IAEG, 2006, pp. 606.

Copyright © Int. J. of GEOMATE All rights reserved, including making copies, unless permission is obtained from the copyright proprietors.
